

Coupled Magnetoelastic Theory of Magnetic and Magnetostrictive Hysteresis

Martin J. Sablik, *Member, IEEE*, and David C. Jiles, *Senior Member, IEEE*

Abstract—A physical model is developed for the coupling between magnetic and magnetostrictive hysteresis and for the effect of mechanical stress on both types of hysteresis. The Jiles-Atherton-Sablik model for magnetomechanical hysteresis is reviewed and interpreted. In that model, under applied stress, the magnetization is coupled to magnetostriction through the derivative of the magnetostriction with respect to magnetization ($d\lambda/dM$). The magnetostriction is also a function of the magnetization even in the absence of stress. An expression for the magnetostriction is derived from minimization of the internal energy with respect to strains, which is necessary for mechanical equilibrium. In the case where stress σ and field H are coaxial and where the material is assumed to be isotropic, the resulting strain consists of a mechanical strain σ/Y , where Y is Young's modulus, and a magnetostrain which goes to zero at saturation (ΔE effect). From the magnetostrain, the magnetostriction is obtained, using the convention that magnetostriction is zero in the unmagnetized state. By taking into account fluctuations in the magnetic energy due to hysteresis, one finds that the magnetostriction initially moves to higher values as the magnitude of the flux density B decreases from its extremum value in λ versus B plots. Also, in a quasi-dc variation of the external field H , the magnetostriction exhibits a nonzero value at the lowest value of its hysteresis loop, although in the unmagnetized state, the magnetostriction is zero. Various numerical cases are evaluated, and the modeling is compared to previous measurements in polycrystalline iron and steel and in terfenol and Ni-Zn ferrites.

I. INTRODUCTION

MAGNETIC hysteresis is a phenomenon which has been known for more than a century [1]–[6]. The behavior is characteristic of ferromagnets, e.g., iron, nickel, cobalt, steels, laves phase intermetallics, and various rapidly-solidified ribbon materials. In a ferromagnet, the magnetic behavior is dependent on the magnetic history of the specimens: that is, on the magnetic fields to which the sample has been exposed. In a typical situation, when the magnetic field is cycled between $+H_{max}$ and $-H_{max}$, the magnetization path followed by the specimen

will be different when the applied field is taken from $+H_{max}$ to $-H_{max}$ than when the field is taken from $-H_{max}$ to $+H_{max}$. On an M versus H plot, a loop will be traced out known as a hysteresis loop which usually will be sigmoidal (slant-S-shaped) in appearance.

For a long time magnetic hysteresis loops could be modeled only by mathematical models which either superposed various mathematical functions [7]–[11] to produce the equivalent of a hysteresis loop, or which reproduced hysteresis loops by building the loops out of much smaller loops, as in the Preisach model [12]–[19]. Another model which could produce hysteresis loops successfully was the Rayleigh model [20], but this applied only to loops in magnetic fields very small compared with the fields which saturate (i.e., fully magnetize) the magnetization. Now, however, a physically based hysteresis model has been developed by Jiles *et al.* [21]–[25] and extended by Sablik *et al.* [26]–[33], to the case of a polycrystalline magnetic material under uniaxial stress aligned with the applied magnetic field. This extended model is able to reproduce magnetic hysteresis loops all the way to saturation [24] while providing a framework for describing the effects of stress on hysteresis [26]. The extended model [30] has been applied to analysis of various magnetomechanical properties (i.e., properties affected by both stress and magnetic field). Examples to which the extended model has been applied are: (1) the effect of stress on higher order harmonics generated by traversal of a low frequency hysteresis loop [27]; (2) the effect of stress on the initial magnetic susceptibility [30], [34]; (3) the effect of stress on hysteresis in the "reversible" permeability [29], [35], the radio frequency (RF) signal absorption [29], and the RF surface resistance [30]; and (4) the effect of stress on the Barkhausen noise amplitude [32] and on the magnetically induced velocity change of ultrasonic waves [32].

The extended model has also been applied to hysteresis in magnetostriction, i.e., hysteresis in the fractional change in length of a magnetic material under an applied magnetic field. An early implementation of the model was able to produce the characteristic butterfly shape of magnetostriction hysteresis, but was lacking in certain details [28]. An energy minimization formulation to obtain an expression for the magnetostriction is used. Prior versions of this formulation have already been discussed [31], [32]. The formulation is modified to make the results consistent

Manuscript received September 17, 1992; revised March 16, 1993. The work in this paper was partly supported by the Electric Power Research Institute, Contract No. RP2426-29 (M. J. Sablik) and by the Department of Energy, Office of Basic Energy Sciences, Division of Material Sciences, contract no. W-7405-ENG-92 (D. C. Jiles). Additionally, internal support was provided by Southwest Research Institute, contract no. 15-9635 (M. J. Sablik).

M. J. Sablik is with the Southwest Research Institute, P.O. Drawer 28510, San Antonio, TX 78228-0510.

D. C. Jiles is with the Ames Laboratory, Iowa State University, Ames, IA 50011.

IEEE Log Number 9209201.

with the conventional understanding of the ΔE effect [33], [36].

The published magnetomechanical hysteresis model [26]–[33] builds on the formulation of Jiles *et al.* [21]–[25]. Thus, three basic inputs enter the model—equilibrium thermodynamics, domain wall translation, and domain wall bowing.

The thermodynamic or anhysteretic expression for the magnetization M_a is derived for a multi-domain system by considering the material to be composed of an array of pseudodomains with fixed domain walls. This consideration is necessary since domain wall translation is an irreversible change and any changes along the anhysteretic curve (which is a locus of thermodynamic equilibrium states) should be reversible. Thus, the net magnetization of each pseudodomain changes by reversible domain moment rotation, as modeled by the anhysteretic magnetization curve. Furthermore, the distribution of domain moments are taken as a canonical ensemble of moments [22], interacting through an effective field. An expression is found for the anhysteretic magnetization in terms of the effective field, the expression for which can be derived from equilibrium thermodynamics [27].

The effective field has a contribution H_σ from the applied stress σ , which causes an adjustment to the magnetization resulting from magnetoelastic coupling. This effect is represented in the expression for H_σ by the factor $d\lambda/dM$, where magnetostriction λ is a nonlinear function of the magnetization. The expression for the anhysteretic magnetization contains two material parameters. The first parameter is a (which is proportional to temperature, domain density, and the inverse of the saturation magnetization). The second parameter is α , the domain coupling parameter. The revised model of the magnetostriction results in an expression for α in terms of Young's modulus, saturation magnetostriction, saturation magnetization, and the elastic constants of the polycrystalline material.

In the hysteresis part of the model, domain wall translation is included as an irreversible contribution to the magnetization. The irreversible magnetization takes the form

$$M_{irr} = M_a - k\delta(\partial M_{irr} / \partial B_e), \quad (1)$$

where parameter $\delta = +1$ or -1 depending on whether H is increasing or decreasing, and where $B_e = \mu_0 H_e$. The constant k is the pinning parameter and is proportional to the domain wall pinning site density and the pinning strength [22], [24]. Since the second term on the right hand side of this equation changes its sign depending on whether H increases or decreases, it acts in opposition to the change in H , analogously to a mechanical friction term. Hence it is seen that irreversibility and hence hysteresis is introduced in a dissipative manner analogous to mechanical friction. The expression (1) can be simplified, resulting in a differential equation that can be solved for the irreversible magnetization. It will be shown that the differential change in the irreversible magnetization will

be a function both of the deviation ($M_a - M_{irr}$) from the anhysteretic magnetization and of the factor $k\delta$, which introduces irreversibility.

In the third part of the model, a term is added to account for the effect of domain wall bowing before unpinning and after repinning of domain walls. Thus, the total magnetization consists of the sum of the irreversible magnetization and the domain wall bowing contribution. The domain wall bowing contribution is also a function of the deviation ($M_a - M_{irr}$) from the anhysteretic magnetization. The parameter c appearing in the domain wall bowing contribution can be shown to be equal to the ratio of the initial normal susceptibility to the initial anhysteretic susceptibility [24] (where "initial" refers to the unmagnetized state).

One basic premise of this model is that through the thermodynamics, magnetization and magnetostriction are inextricably coupled. Our original models have been generalized here because the expressions that we have used for the magnetostriction in the past [26]–[30], [34] were ad hoc.

An expression for the magnetostriction is derived from magnetoelastic considerations, using a multi-domain model is shown. Derivation of magnetostriction as a function of stress and magnetization results from considering the system in mechanical equilibrium. In our derivation, the internal energy—consisting of elastic terms, magnetoelastic terms and magnetic terms—is minimized with respect to the strains. Under the simplifying assumption that the polycrystalline system is isotropic, and after appropriate integration, the equilibrium magnetostriction is extracted by formulating the equilibrium mechanical strain. Some of the magnetic terms in the internal energy are hysteretic terms because they are functions of the deviation of the magnetization from the anhysteretic magnetization. The multi-domain nature of the model arises because the formulation is in terms of macroscopic magnetization and magnetostriction which takes into account the multi-domain nature of the material. The theory is applied specifically to polycrystalline steels.

Details of the mathematics of the theory are presented in Sections II and III. Section II describes the existing theory of magnetomechanical hysteresis [21]–[30]. We present the original restricted theory for the sake of completeness, and also for the purpose of clarification of certain points. Section III describes the extended theory, in which an expression for magnetostriction is developed as a function of stress and magnetization. In Section IV, generic results are presented for polycrystalline steel and compared to experimental behavior in polycrystalline steel published previously.

II. MATHEMATICAL DESCRIPTIONS OF EXISTING MAGNETOMECHANICAL HYSTERESIS MODEL

In the anhysteretic state, which describes thermodynamic equilibrium, the polycrystalline ferromagnet is treated [21], [22] as a canonical ensemble of interacting

magnetic domains each carrying a magnetic moment \vec{m} . The distribution of domains at temperature T carries a total magnetization M in the field direction given by

$$M = \frac{\int_0^\pi M_s \cos \theta e^{-E_d(\theta)/k_B T} \sin \theta d\theta}{\int_0^\pi e^{-E_d(\theta)/k_B T} \sin \theta d\theta} \quad (2)$$

where θ is the angle between domain moment \vec{m} and applied field \vec{H} , and where $M_s = Nm$ is the saturation magnetization of N domains per unit volume. $E_d(\theta)$ is the domain energy in the presence of the other domains and in the presence of an external field H . The effect of interaction between domains can be represented as an effective contribution to the magnetic field, and so

$$E_d(\theta) = -\mu_o m H_e \cos \theta. \quad (3)$$

where the effective field H_e is [26]

$$H_e = H + \alpha M + H_\sigma. \quad (4)$$

The contribution αM to the effective field arises from magnetic interaction between domains [24] and the contribution H_σ from the presence of stress σ arises from magnetoelastic interaction between domains. An expression for coupling parameter α will be derived later in Section III in terms of the saturation magnetostriction, elastic constants, and saturation magnetization. From thermodynamics [27] it follows that in the case of coaxial stress and field,

$$G = U - TS + (3/2)\sigma\lambda, \quad (5a)$$

$$U = (1/2)\alpha\mu_o M^2, \quad (5b)$$

$$A = G + \mu_o H M. \quad (5c)$$

where G is the Gibbs free energy density, U is the internal energy density, and A is the Helmholtz free energy density. It then follows that the effective field H_e is [27]

$$H_e = \frac{1}{\mu_o} \left(\frac{\partial A}{\partial M} \right)_T = H + \alpha M + \frac{3}{2} \frac{\sigma}{\mu_o} \left(\frac{\partial \lambda}{\partial M} \right)_T. \quad (6)$$

Comparing with (4), it is found that

$$H_\sigma = \frac{3}{2} \frac{\sigma}{\mu_o} \left(\frac{\partial \lambda}{\partial M} \right)_T, \quad (6a)$$

where λ is the bulk magnetostriction under applied field H . If one carries out the integration in (2), then defining $a = Nk_B T / \mu_o M_s$, one obtains [21]–[24]

$$M = M_s \mathcal{L}(H_e/a) \equiv M_a, \quad (7)$$

where $\mathcal{L}(x) = \coth(x) - 1/x$ is the Langevin function. The assumption is made here that domain density N remains constant. In other words, domain wall motion is not considered. This is consistent because we are considering here only reversible changes along the thermodynamic (anhysteretic) path. Such changes can only involve rotation of domain moments because domain wall motion is

dissipative. Hence domain density should be effectively constant in the processes under consideration.

It was mentioned in the introduction that the domains discussed in this part of the development should be considered pseudodomains. One reason is the restriction that the domain walls are not allowed to move. A second reason is that the average volume, $1/N$, of these pseudodomains is smaller than that of real domains. The average pseudodomain diameter computed for $a = 3000$ (a typical value used for a) is about 9 nm at 300 K. For real domains in iron, the domain walls are 40 nm thick [37], and the domains of course are much larger in extent. Nevertheless, using the concept of pseudodomains, it is found that (7) gives a good description of the experimentally determined anhysteretic magnetization curve [21]–[25].

The parameter a should be treated as a constant of the material dependent in part on microstructure. Equation (7) is the expression used for the anhysteretic magnetization M_a , since it was derived under the assumption of thermal equilibrium.

Next to be considered is the irreversible contribution to the magnetization which arises because of domain wall motion. The motion of domain walls is impeded by the presence of pinning sites. Energy is lost to the lattice as the domain walls pin and unpin in the increasing field. As shown by Jiles *et al.* [21]–[25] the energy dissipation can be characterized by energy density.

$$E_{pin}(M) = k \int_0^M dM. \quad (8)$$

where k is known as the pinning constant and is a microstructural parameter proportional to the pinning site density and pinning site energy. The reversible increase in energy density that would occur if no energy were dissipated is $\int_0^M M_a(H_e) dB_e$, (where $B_e = \mu_o H_e$), and the total energy density increase is

$$\int_0^M M dB_e = \int_0^M M_a dB_e - k \int_0^M \left(\frac{dM}{dB_e} \right) dB_e. \quad (9)$$

Differentiating with respect to B_e then yields

$$M = M_a - \delta k \left(\frac{dM}{dB_e} \right), \quad (9a)$$

which has been previously written as (1). The parameter δ takes the value $+1$ when H increases and -1 when H decreases, since pinning always impedes the effect of whatever is the change in the external field. Equation (9a) may be manipulated to a more convenient form as [24], [27]

$$\frac{dM}{dH} = \frac{(M_a - M)}{\frac{\delta k}{\mu_o} - \left(\alpha + \frac{3}{2} \frac{\sigma}{\mu_o} \left(\frac{\partial^2 \lambda}{\partial M^2} \right)_T \right) (M_a - M)}. \quad (10)$$

The M written here is the irreversible expression for the magnetization, and is to be henceforth denoted as M_{irr} .

Hysteresis is built into the model via the parameters δ and k , and thus the magnetization M_{irr} behaves differently when H is increasing than when H is decreasing. Thus, as H increases from zero to H_{max} , the magnetization M_{irr} follows an initial magnetization curve to M_{max} ; when H decreases to $-H_{max}$, the magnetization M_{irr} follows the top part of the magnetic hysteresis loop; when H then increases to H_{max} , the magnetization M follows the bottom part of the hysteresis loop; and as H continues to vary between H_{max} and $-H_{max}$, the magnetization M_{irr} continues to follow the hysteresis loop already traced. The hysteresis loop changes to a new loop when H increases beyond H_{max} to H'_{max} and $-H'_{max}$. In fact, all of the quantitative hysteretic behavior usually seen in ferromagnets can be seen in the hysteresis loop followed by M_{irr} . Note that, mathematically, M_{irr} is computed via integration over an expression which is a function of the deviation ($M_a - M_{irr}$) from the anhysteretic magnetization.

The integration is also carried out in such a way that dM is set to zero whenever the sign of the derivative dM_{irr}/dH is negative. Because of this last constraint, the history of the hysteresis enters in a "globally" dependent way rather than in a "local" way. This means that the solution is not mathematically unique for each local hysteretic reversal, but rather depends on the global history of the sample before the hysteretic reversal.

A better quantitative fit is obtained if one includes in the physical description the property of the bending (bowing) of domain walls before their becoming unpinned. Jiles and Atherton [24] discuss this feature and arrive at an expression for the total hysteretic magnetization as

$$M = M_b + M_{irr} \quad (11)$$

where M_b is the bowing contribution derived from a microstructural argument which takes into account changes in magnetization as domain walls bow out from an unbowed shape. In past work, [21]–[25] M_b has also been described by the symbol M_{rev} because bowing occurs without energy dissipation. The resultant expression for M_b is [24]

$$M_b = c(M_a - M_{irr}), \quad (11a)$$

where c is the ratio of the initial magnetic susceptibility (determined from the slope of the initial normal magnetization curve of M extrapolated to $H = 0$) to the initial anhysteretic susceptibility (determined from the slope of the anhysteretic magnetization M_a curve extrapolated to $H = 0$). Note that M_b is also in terms of the deviation ($M_a - M_{irr}$) from the anhysteretic magnetization.

Some of the characteristics of this model are that pinning parameter k primarily determines the coercivity H_c of the hysteresis loop and that parameters α and a primarily affect the slope of the hysteresis curve. The presence of stress σ shifts the slope of the hysteresis curve because of the additional contribution to the effective field. For a material with positive $d\lambda/dM$, the slope increases under positive stress (tension); under negative stress

(compression), the slope decreases [26]. Change in σ has an opposite effect however on the coercivity [32], with coercivity decreasing with increasing tension, and vice-versa with compression. The shift in slope comes about because the term H_a to first order can be written as $\bar{\alpha}M$ and thus the stress adds an additional contribution to α , which as we have noted, affects the slope of the hysteresis curve [26], [27].

The magnetostriction λ is a function of M [26]–[28], and in Section III, a derivation is proposed for λ in terms of energy minimization arguments. In the past, several different *ad hoc* functions were used for λ [26]–[28]. Precise variation of the slope of the magnetic hysteresis curve with stress is determined by $\lambda(M)$. Since M exhibits hysteresis, so also does $\lambda(M)$, which depends on M . The hysteresis in $\lambda(M)$ versus H , characterized by a butterfly-shaped loop, generally displays reflection symmetry about the ordinate λ axis [28], [34], [38]. A somewhat similarly shaped (butterfly-like) loop is also seen in λ versus B loops [28].

From (4), (6), and (7), it is seen that when $\sigma \neq 0$, the magnetostriction and magnetic hysteresis are mutually coupled. These features have been previously noted by Sablik *et al.* [28], [32].

III. DERIVATION OF THE MAGNETOSTRICTION FROM THE INTERNAL ENERGY

The internal energy density of a ferromagnetic polycrystalline material is expressed as

$$E = E_{el} + E_{me} + \phi_{mag}, \quad (12)$$

where if the field and stress are in the z direction.

$$E_{el} = \frac{1}{2}c_{11}(e_{xx}^2 + e_{yy}^2 + e_{zz}^2) + \frac{1}{2}c_{44}(e_{xy}^2 + e_{yz}^2 + e_{zx}^2) + c_{12}(e_{yy}e_{zz} + e_{yy}e_{xx} + e_{xx}e_{zz}) - e_{zz}\sigma, \quad (13a)$$

$$E_{me} = b \sum_i e_{ii}(\alpha_i^2 - \frac{1}{3}) = \frac{2}{3}b e_{zz} - \frac{1}{3}b(e_{xx} + e_{yy}) \quad (13b)$$

$$\phi_{mag} = U_{mag} + \phi_{hys} = \frac{1}{2}\alpha\mu_o M^2 + f(M - M_a). \quad (13c)$$

The term E_{el} is the elastic energy density expressed in terms of strains e_{ij} . The polycrystalline system is assumed to be isotropic and not grain-oriented, so that a constraint relationship exist among the elastic constants, namely

$$c_{44} = (c_{11} - c_{12})/2. \quad (14)$$

The term E_{me} is the magnetoelastic energy density, expressed in terms of isotropic magnetoelastic coupling constant b . In (13b) for E_{me} , it is taken that the direction cosines of the magnetization are $\alpha_1 = 0$, $\alpha_2 = 0$, $\alpha_3 = 1$, since in an isotropic system the magnetization is aligned with the field. The magnetic energy density ϕ_{mag} consists of two terms: (a) the thermodynamic internal energy density U_{mag} arising from internal coupling between the domains and is given as $(1/2)\alpha\mu_o M^2$, and (b) a separate hysteretic energy density term ϕ_{hys} which is a function of

the deviation of the magnetization from the anhysteretic magnetization.

Minimizing with respect to the strains for mechanical equilibrium, following a procedure similar to that of Spano *et al.* [39], one finds that [31]–[33]

$$\begin{aligned} \partial E / \partial e_{xx} &= c_{11} e_{xx} + c_{12} (e_{yy} + e_{zz}) \\ &+ \partial \phi_{mag} / \partial e_{xx} - b/3 = 0, \end{aligned} \quad (15a)$$

$$\begin{aligned} \partial E / \partial e_{yy} &= c_{11} e_{yy} + c_{12} (e_{xx} + e_{zz}) \\ &+ \partial \phi_{mag} / \partial e_{yy} - b/3 = 0, \end{aligned} \quad (15b)$$

$$\begin{aligned} \partial E / \partial e_{zz} &= c_{11} e_{zz} + c_{12} (e_{xx} + e_{yy}) \\ &+ \partial \phi_{mag} / \partial e_{zz} - \sigma + (2/3)b = 0. \end{aligned} \quad (15c)$$

$$\partial E / \partial e_{xy} = c_{44} e_{xy} + \partial \phi_{mag} / \partial e_{xy} = 0, \quad (15d)$$

$$\partial E / \partial e_{xz} = c_{44} e_{xz} + \partial \phi_{mag} / \partial e_{yz} = 0, \quad (15e)$$

$$\partial E / \partial e_{yz} = c_{44} e_{yz} + \partial \phi_{mag} / \partial e_{yz} = 0. \quad (15f)$$

In an isotropic system, $e_{xy} = e_{yz} = e_{zy} = 0$ and hence from (15d)–(15f), it follows that

$$\partial \phi_{mag} / \partial e_{xy} = \partial \phi_{mag} / \partial e_{xz} = \partial \phi_{mag} / \partial e_{yz} = 0. \quad (16)$$

One may now apply the result for an isotropic system that

$$e_{xx} = e_{yy} \equiv e_{\perp} = -\nu e_{zz}, \quad (17)$$

where ν is Poisson's ratio, given by

$$\nu = c_{12} / (c_{11} + c_{12}). \quad (18)$$

Equations (15a) and (15b) then lead to the relationships that

$$\partial \phi_{mag} / \partial e_{xx} = b/3$$

and

$$\partial \phi_{mag} / \partial e_{yy} = b/3,$$

which, after integration, sum to

$$\phi_{mag} = (b/3)(e_{xx} + e_{yy}) + f_{\perp}(e_{zz}), \quad (19a)$$

where $f_{\perp}(e_{zz})$ is a function which is determined after integrating (15c). Integration of (15c) with respect to e_{zz} yields

$$\begin{aligned} \frac{1}{2}(c_{11} - 2c_{12}\nu)e_{zz}^2 - (\sigma - (2/3)b)e_{zz} + \phi_{mag} \\ + f_z(e_{xx}, e_{yy}) + c_z = 0. \end{aligned} \quad (19b)$$

Equations (19a) and (19b) reduce to one equation after appropriate replacements for f_{\perp} and f_z . This single equation is

$$\begin{aligned} \frac{1}{2}(c_{11} - 2c_{12}\nu)e_{zz}^2 - (\sigma - (2/3)b(1 + \nu))e_{zz} \\ + \phi_{mag} + c_z = 0. \end{aligned} \quad (20)$$

In arriving at (20), we have used (17).

To solve for the magnetostriction, one uses the result that Young's modulus for the isotropic case is [38]

$$Y = \frac{(c_{11} - c_{12})(c_{11} + 2c_{12})}{c_{11} + c_{12}} = c_{11} - 2c_{12}\nu, \quad (21)$$

so that (20) becomes

$$\begin{aligned} e_{zz} = \frac{\sigma}{Y} - \frac{2}{3} \frac{b(1 + \nu)}{Y} \pm \left\{ \left[\frac{1}{Y} \left(\sigma - \frac{2}{3} b(1 + \nu) \right) \right]^2 \right. \\ \left. - \frac{2}{Y} (\phi_{mag} + c_z) \right\}^{1/2}. \end{aligned} \quad (22)$$

The term σ/Y is the mechanical strain and the rest is the magnetostrain e_{me} . To evaluate constant of integration c_z , one recalls from Cullity [36] that the ΔE effect is understood by postulating that at saturation, $e_{zz} = \sigma/Y$ and the magnetostrain is zero. Thus, one solves for c_z by setting $e_{me} = 0$ at saturation, where both M and M_a equal M_s . Thus, at saturation,

$$\begin{aligned} 0 = -\frac{2}{3} \frac{b(1 + \nu)}{Y} \pm \frac{1}{Y} \{ (\sigma - (2/3)b(1 + \nu))^2 \\ - 2Y(c_z + \phi_{mag}(M_s)) \}^{1/2} \end{aligned}$$

or

$$\begin{aligned} c_z = (1/2Y) \{ (\sigma - (2b(1 + \nu)/3))^2 \\ - (2b(1 + \nu)/3)^2 \} - \phi_{mag}(M_s). \end{aligned} \quad (23)$$

Thus, the magnetostrain is

$$\begin{aligned} e_{me} = -\frac{2}{3} \frac{b(1 + \nu)}{Y} + \frac{2}{3} \frac{b(1 + \nu)}{Y} \{ 1 - \\ (9Y/2b^2(1 + \nu)^2) (\phi_{mag}(M) - \phi_{mag}(M_s)) \}^{1/2}. \end{aligned} \quad (24)$$

The plus sign is chosen to have $e_{me} = 0$ when $M = M_s$.

The conventionally defined magnetostriction λ varies differently than the magnetostrain itself. In particular, λ is usually defined as zero in the unmagnetized state and is λ_s , the saturation magnetostriction, at saturation. Thus, we write

$$\frac{3}{2}\lambda = e_{me}(M) - e_{me}^0, \quad (25)$$

where the incorporation of the $3/2$ factor follows Chikazumi and Charap [40] and where e_{me}^0 is the magnetostrain in the unmagnetized state. It should be clear that (25) leads to $\lambda = 0$ when $M = M_a(H = 0) = 0$ and $\lambda = \lambda_s = -(2/3)e_{me}^0$ when $M = M_s$. For polycrystalline steel with b negative [41], it is seen that λ_s is positive, according to (25). Using (24), one finds that

$$\begin{aligned} \frac{3}{2}\lambda = -\left(\frac{2}{3} \frac{b(1 + \nu)}{Y} \right) \left[\left\{ 1 + \left(\frac{9Y}{2b^2(1 + \nu)^2} \right) \right. \right. \\ \cdot \phi_{mag}(M_s) \}^{1/2} - \left\{ 1 + \left(\frac{9Y}{2b^2(1 + \nu)^2} \right) \right. \\ \cdot [\phi_{mag}(M_s) - \phi_{mag}(M)] \}^{1/2} \right]. \end{aligned} \quad (26)$$

Equation (26) for the magnetostriction can be used to evaluate magnetic coupling parameter α , first introduced in (6) for effective field H_e . In particular, at saturation, M

$$= M_a = M_s \text{ and}$$

$$\phi_{mag} = (1/2)\mu_o\alpha M_s^2.$$

Substituting into (26), it is found that at saturation,

$$\frac{3}{2}\lambda = \frac{3}{2}\lambda_s = -[(2b(1+v)/3Y)\left\{1 + \left(\frac{3Y}{2b(1+v)}\right)^2 \cdot \frac{\alpha\mu_o}{Y} M_s^2\right\}^{1/2} - 1] = -(2b(1+v)/3Y)\gamma. \quad (27)$$

If one also writes [41]

$$\begin{aligned} \lambda_s &= \bar{\lambda} = -2b/(3(c_{11} - c_{12})) \\ &= -\frac{2}{3}(2b(1+v)/3Y)\gamma, \end{aligned} \quad (28)$$

then from (21),

$$\begin{aligned} \frac{2}{3}(1+v)\gamma &= Y/(c_{11} - c_{12}) \\ &= (c_{11} + 2c_{12})/(c_{11} + c_{12}). \end{aligned} \quad (29)$$

Also, from (27),

$$\gamma = \left\{1 + \frac{4\gamma^2\mu_o M_s^2}{9\lambda_s^2 Y}\alpha\right\}^{1/2} - 1,$$

and

$$\alpha = \{9Y\lambda_s^2/[4\mu_o M_s^2]\} \{(\gamma + 2)/\gamma\}. \quad (30)$$

Thus, in this extended version of the model, α is not a free parameter, but is completely determined experimentally through (29) and (30). Note that (30) results from considering the material at saturation.

The model to be used for the hysteretic energy density ϕ_{hys} is

$$\phi_{hys} = \frac{1}{2}\mu_o\alpha''(M_a - M)^2 - \mu_o\alpha'(M_a - M)H. \quad (31)$$

where the two terms are obtained by insertion of $\Delta M = M_a - M$ in place of M in the internal energy density term and in the external energy density term dependent on H . This is in effect a magnetic fluctuation energy density owing to hysteresis. Just as in earlier hysteretic expression, this term is expressed in terms of a deviation of the form $M_a - M$. The two parameters, α'' and α' , can be obtained experimentally.

The hysteretic term involving α'' is needed in order to reproduce the "lift-off" phenomenon, i.e., it is found experimentally [28], [38] that after the magnetostriction varies from zero as the system initially magnetizes, the magnetostriction does not return to zero at any time when the field cycles through the ensuing magnetostrictive hysteresis loop [28], [32], [33]. The value λ_{min} of the magnetostriction at the minimum point of the magnetostriction loop has been addressed as the "lift-off" value of the magnetostriction loop. The term involving α'' in (31) primarily produces this behavior.

The hysteretic term involving α' results in the correct sequence of cycling around the λ versus B loop. Without this term, the modeling of λ versus B does not exhibit hysteresis. Another approach [28] that has been tried for

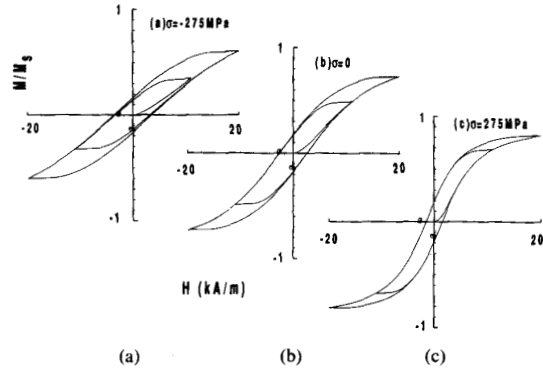


Fig. 1. Magnetization hysteresis curves computed for stresses of (a) -275 MPa, (b) 0 MPa, and (c) +275 MPa, where negative stress is compressive and positive stress is tensile. Magnetization is normalized by saturation magnetization M_s . Note that, as stress σ goes from negative to positive, the loop narrows, the slope increases, and the interior loops increase in size. For this calculation, $M_s = 1.61 \times 10^6$ A/m, $a = 4500$ A/m, $k/\mu_o = 3000$ A/m, $c = 0.1$, $c_{11} = 1.26 \times 10^8$ kN/m², $c_{12} = 4.8 \times 10^7$ kN/m², $b = -0.242 \times 10^8$ kN/m², $\alpha' = 7.5 \times 10^{-4}$, and $\alpha'' = 3.5 \times 10^{-5}$. This yields $\lambda_s = 20.7 \times 10^{-6}$ and $\alpha = 6.87 \times 10^{-5}$.

the magnetostriction has expressed the magnetostriction as a function of effective field H_e . This was able to produce hysteresis in λ versus B , but when B reached its maximum, the magnetostriction did not at first continue to increase as B started decreasing, which is a characteristic of the experimentally observed λ versus B loops [28]. With the α' term in (13c) and (31), the magnetostriction as expressed by (26) shows the experimentally observed [28], [32] cycling behavior around the loop. The fact that λ continues to increase as B and H decrease is a reflection of magnetostrictive hysteresis being subsidiary to magnetic hysteresis.

Note that in (7) for the anhysteretic magnetization, the hysteretic terms in λ do not contribute to $(d\lambda/dM)_T$, since $M - M_a$ is zero in the thermodynamic expression for λ . Neither do the hysteretic terms in λ contribute to $(d^2\lambda/dM^2)_T$ in (10) because this derivative originates from the derivative dB_e/dM and B_e , from above, depends only on M_a , not M . Thus, the hysteretic terms in λ are important only for correctly obtaining the total magnetostriction after correctly obtaining the total magnetization.

It is possible to measure parameters α' and α'' experimentally. Parameter α'' is obtained from magnetostriction retentivity λ_r at $H = 0$ in the saturation loop. Parameter α' is obtained from the coercivity H_c and the values $\lambda(H_c, M = 0)$ and $M_a(H_c, M = 0)$ for the saturation loop.

IV. MODELING RESULTS AND COMPARISON WITH EXPERIMENTAL RESULTS

Fig. 1 shows a magnetic hysteresis curve calculated from the model for the constant stress conditions of $\sigma = -275, 0, +275$ MPa (i.e., -40, 0, +40 ksi) for polycrystalline steel. Negative stress means compression and positive stress means tension. Fig. 2 shows λ versus H hysteresis curves; Fig. 3 shows λ versus B hysteresis curves. Both sets of magnetostriction hysteresis curves are

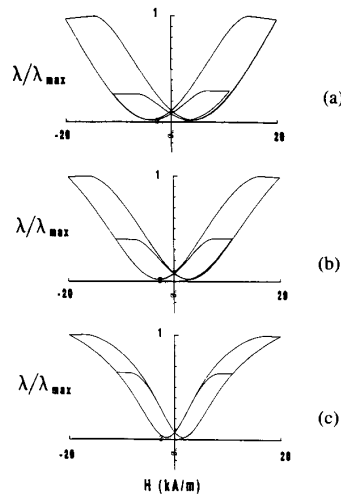


Fig. 2. Magnetostriction hysteresis curves (λ versus H) computed for stresses of (a) -275 MPa, (b) 0 MPa, and (c) $+275$ MPa. Magnetostriction is normalized in each case by its maximum value of 5.40×10^{-6} , 8.67×10^{-6} , and 11.56×10^{-6} , respectively, for the three cases of stress. Note that liftoff is largest for tension. In going from compression to tension, the loops narrow and the interior loops increase in amplitude. Parameter values here are the same as in Fig. 1.

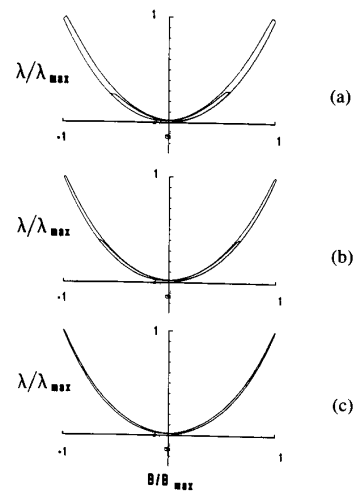


Fig. 3. Magnetostriction λ versus flux density B computed for stresses of (a) -275 MPa, (b) 0 MPa, and (c) $+275$ MPa, with parameter values unchanged. Flux density is normalized by its maximum value B_{max} in each case. Again, $\alpha' = 0.75 \times 10^{-3}$, $\alpha'' = 3.5 \times 10^{-5}$.

for stress $\sigma = -275$, 0 , and $+275$ MPa. For these curves, $\alpha' = 0.00075$ and $\alpha'' = 0.000035$ were used. A complete listing of other parameters used may be found in the figure captions. Note that the application of uniaxial tensile stress coaxial with the field increases liftoff and narrows the hysteresis in polycrystalline steel; compression does the opposite. In the case of magnetic hysteresis, tension primarily increases the slope (susceptibility) of the hysteresis; compression does the opposite. Note that coupling parameter α is smaller than in the early models [21]–[30]: this means that the slope of the hysteresis curve is

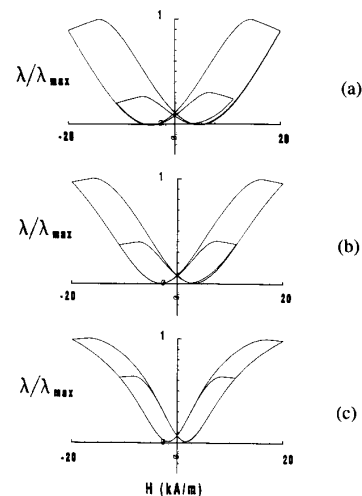


Fig. 4. Magnetostriction hysteresis for λ versus H computed for $\alpha' = 1.25 \times 10^{-3}$, where α'' and the other parameters are the same as in previous figures. Magnetostriction is normalized in each case by its maximum value of 5.12×10^{-6} , 8.52×10^{-6} , and 11.48×10^{-6} for (a) -275 MPa, (b) 0 MPa, and (c) $+275$ MPa, respectively. Increasing α' here widens the loops and reduces liftoff.

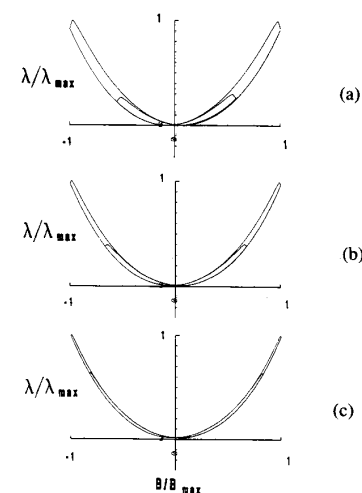


Fig. 5. Magnetostriction hysteresis for λ versus B computed for (a) -275 MPa, (b) 0 MPa, and (c) $+275$ MPa and for $\alpha' = 1.25 \times 10^{-3}$ as in Fig. 4.

determined primarily by parameter a , which depends on domain density at zero magnetization, temperature, and saturation magnetization.

In the magnetization calculation, $d\lambda/dM$ and $d^2\lambda/dM^2$ are evaluated for $M = M_a$, and therefore magnetization does not depend on α' and α'' . Thus α' and α'' only influence the magnetostriction hysteresis, and these effects can be studied independently of changes in the magnetization hysteresis.

Figs. 4 and 5 show λ versus H and λ versus B for $\alpha' = 0.00125$; all other parameters are as before. Note that

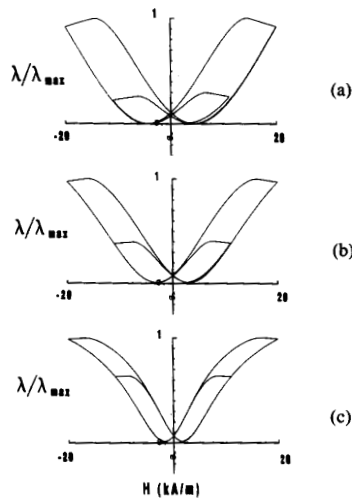


Fig. 6. λ versus H loops computed for $\alpha' = 1.50 \times 10^{-3}$ and other parameters as earlier. This time the λ_{max} values are 4.98×10^{-6} , 8.44×10^{-6} , and 11.45×10^{-6} for (a) -275 MPa, (b) 0 MPa, and (c) +275 MPa, respectively.

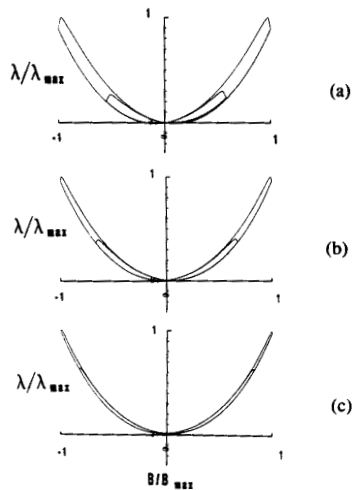


Fig. 7. λ versus B loops computed for (a) -275 MPa, (b) 0 MPa, and (c) +275 MPa and $\alpha' = 1.50 \times 10^{-3}$ as in Fig. 6.

increasing α' has the effect of widening the magnetostriction loops; the effect is particularly noticeable for the λ versus B loops. Liftoff is also reduced to the point where under 40 ksi of compression, there is no liftoff.

As seen in Figs. 6 and 7, for $\alpha' = 0.00150$, the liftoff, in the case of compression, can become negative. Note that the α' has the effect of modifying liftoff in addition to controlling the widths of the magnetostriction loops.

Figs. 8 and 9 show the effect of greatly increasing α'' to 0.00135. In this case, which is also for $\alpha' = 0.00125$, the liftoff is dramatically increased and its behavior with stress is now modified so that liftoff in this case is greater

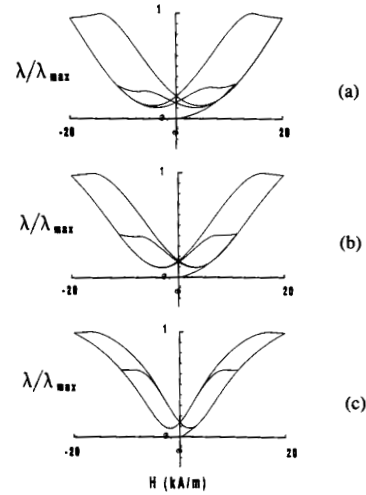


Fig. 8. λ versus H loops computed for $\alpha' = 1.25 \times 10^{-3}$ and for $\alpha'' = 1.35 \times 10^{-4}$ with other parameters as before. Here, $\lambda_{max} = 5.33 \times 10^{-6}$, 8.57×10^{-6} and 11.50×10^{-6} , respectively for (a) -275 MPa, (b) 0 MPa, and (c) +275 MPa. With the increase in α'' , liftoff is enhanced; also dependence of liftoff on stress is altered, so that liftoff is now less for tension.

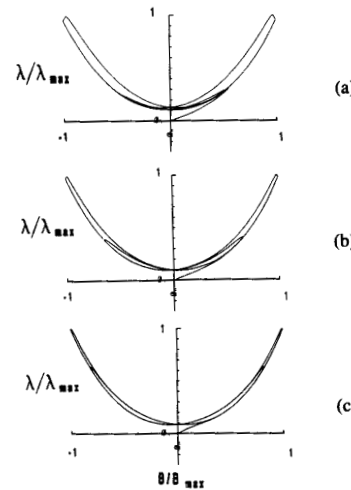


Fig. 9. λ versus B loops computed for (a) -275, (b) 0 MPa, and (c) +275 MPa and for $\alpha' = 1.25 \times 10^{-3}$ and $\alpha'' = 1.35 \times 10^{-4}$.

with compression than with tension. Thus, both types of liftoff dependence on stress are possible—that is, there can be an increase or a decrease of magnetostriction liftoff with compression.

Figs. 10, 11, and 12 show magnetization and magnetostriction hysteresis for a case where material parameters M_s , k , and a are changed to $M_s = 1.25 \times 10^6$ A/m, $k/\mu_0 = 7000$ A/m, and $a = 3150$ A/m. In this case, as seen in Fig. 10, the changes in the magnetization hysteresis are more extreme than in Fig. 1 as the applied stress is changed from compression to tension. In correspondence with the large value of k , there is a large decrease in

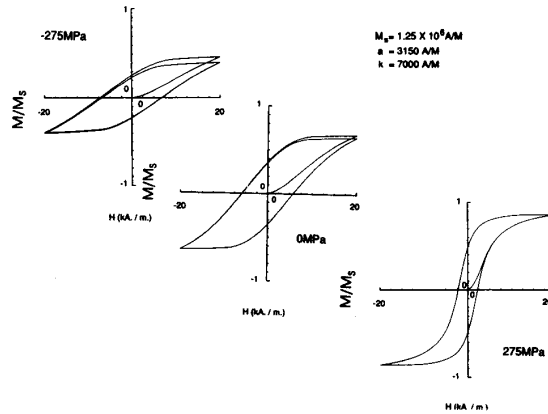


Fig. 10. Magnetization hysteresis M versus H computed for three cases of applied stress ($\sigma = -275$ MPa, $\sigma = 0$, $\sigma = +275$ MPa) and with $M_s = 1.25 \times 10^6$ A/m, $k/\mu_o = 7000$ A/m, $a = 3150$ A/m, $\alpha' = 1.25 \times 10^{-3}$, and $\alpha'' = 3.5 \times 10^{-5}$.

the coercivity as the stress is changed from compression to tension. Similarly, in correspondence with the smaller value of a , there is a large increase in remanence and magnetic susceptibility (slope of the M versus H hysteresis curve) as compression changes to tension. Even more striking is the predicted behavior of λ versus H in Fig. 11, where the magnetostriction hysteresis loops are much wider than those shown earlier, and where the loop shape under tension is distinctively different from the loop shape under compression, tending to be concave inward rather than concave outward. This distinctive shape in part corresponds to the smaller value of M_s , and tends to be less noticeably apparent for larger values of M_s . The λ versus B loops, seen in Fig. 12, for these new values of the material parameters, are generally wider in shape, particularly for zero field or for compressive conditions. The phenomena of (1) liftoff and (2) continuing increase of λ as B decreases from its maximum value are still seen, as before. In this case, the figures do not show interior loops, and hence one additional phenomena is made much more noticeably clear. This additional phenomenon is that during initial magnetization, the magnetization and magnetostriction may rise to different values than the values to which they return after traversing a full loop. This phenomenon is often seen experimentally, although it is not always present, and would be worthy of additional study in a later work.

The generic behavior of the magnetostriction hysteresis, as described above, can be seen experimentally not only in the behavior of steel and polycrystalline iron but also in other materials such as Terfenol D [38] and Ni-Zn ferrites [42]. Magnetostriction hysteresis in Terfenol D was reported by Jiles and Hariharan [38] and may be seen in Fig. 2 of that paper. It is seen that for that material, the description of magnetostriction with liftoff decreasing with compressive stress is the applicable one. Bienkowski and Kulikowski [42] report magnetostriction hysteresis for Ni-Zn ferrites in Fig. 4 of their paper. In

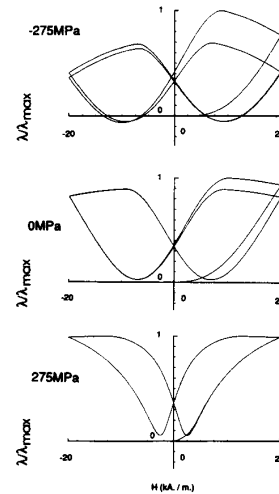


Fig. 11. λ versus H loops computed for the same values of M_s , k/μ_o , a , α' , and α'' as in Fig. 10. Here we have $\lambda_{max} = 1.23 \times 10^{-6}$, 5.80×10^{-6} and 13.02×10^{-6} and for $\sigma = -275$ MPa, 0 MPa, and 275 MPa, respectively.

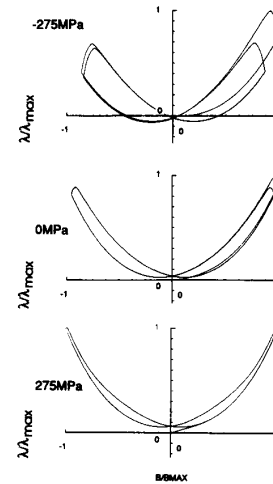


Fig. 12. λ versus B loops computed for -275 , 0 , $+275$ MPa and for the same values of the material parameters as in Figs. 10 and 11.

this case, magnetostriction is negative and the hysteresis appears as a butterfly curve which reflected across the $\lambda = 0$ axis. Liftoff is again seen in that the negative magnetostriction does not return to zero after the material leaves the demagnetized state. Bienkowski and Kulikowski [42] report magnetostriction hysteresis only for unstressed material.

The results for the model compare favorably with experimental results for unstressed steel and polycrystalline iron at low fields. [See Figs. 1 and 2 in [28], and Fig. 13 here]. Clearly seen in all the experimental magnetostriction hysteresis displayed is the liftoff phenomenon. The λ versus B (See [28] and Fig. 13) plots clearly show hysteresis as well as the phenomenon of λ increasing imme-

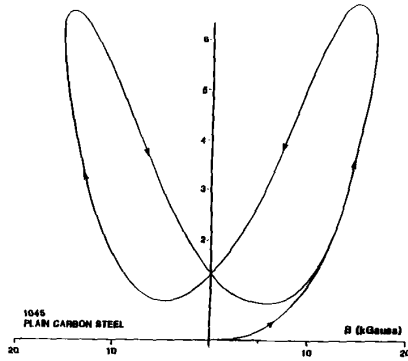


Fig. 13. Experimental magnetostriction hysteresis (λ versus B) for polycrystalline steel (1045 plain carbon steel containing 0.45 wt. % carbon). The specimen was not subject to applied stress.

diately after B reaches a maximum and starts decreasing. The λ versus H plot in [28] for polycrystalline iron is more characteristic of the plots in Fig. 11, showing large magnetostriction hysteresis and showing also the behavior of not returning to the same value after traversing a full magnetostriction hysteresis loop. Similarly, the λ versus B loops for polycrystalline iron and steel tend to be more open, like the loops in Fig. 12.

At higher fields H , the behavior of the magnetostriction hysteresis in iron and steel is a little more complicated experimentally. Magnetostriction hysteresis for 2% Mn pipeline steel is reported by Atherton *et al.* [43] (See Figs. 1, 2, and 3 in [43]). The λ versus H and λ versus M curves for $\sigma = 100$ MPa all show liftoff behavior. Furthermore, the λ versus H curves for the pipeline steel greatly resemble our curves except for a slight falloff in magnetostriction values for H greater than 7.5 kA/m. The λ versus M curves ought to behave like λ versus B curves because of the high permeability, which ensures that $B \approx \mu_0 M$. However, the experimental λ versus M curves have three crossovers between the upper and lower branches of the hysteresis loop. The extra crossovers may be associated with decrease in magnetostriction at the higher fields and hysteretic influences due to that decrease. It is known [44] that polycrystalline iron at high enough fields show such a large reduction in the magnetostriction (as a result of the Ewing-Villari effect [45]–[47]) that the magnetostriction eventually goes negative. Presumably the pipeline steel reflects some of these tendencies.

This change in sign of $d\lambda/dH$ at the higher fields in polycrystalline iron (and steel) might be extracted from (26) if the magnetoelastic coupling constant b for the polycrystalline system can be represented as a function of the magnetization. As mentioned earlier in (28), Chikazumi [40] represents b as

$$b = -(3\bar{\lambda}/2)(c_{11} - c_{12}) = -3\bar{\lambda}C_{44} \quad (32)$$

for an isotropic polycrystalline system, where $\bar{\lambda}$ is

$$\bar{\lambda} = \frac{2}{3}\lambda_{100} + \frac{1}{3}\lambda_{111}, \quad (33)$$

where λ_{100} is the saturation magnetostriction with the

magnetic aligned along the $[100]$ axis and λ_{111} is for the case of magnetic moments aligned along the $[111]$ axis. In crystalline iron, λ_{100} is positive and λ_{111} is negative.

To represent polycrystalline iron, a model could be constructed so that the domains in polycrystalline iron are such that at first their moments tend to be along the $\langle 100 \rangle$ directions in the respective crystal grains in the polycrystal. Then as magnetization increases, the domains with moments tending to be aligned in the $\langle 111 \rangle$ direction of the crystallites grow at the expense of other domains. The net result is that domains with negative magnetostriction would tend to dominate; b in turn would change from negative to positive; and bulk magnetostriction, which is an average of all the domain magnetostrictions, would change from positive to negative.

V. CONCLUSION

We have demonstrated that hysteresis in the magnetostriction λ is coupled to hysteresis in the magnetization M because of the dependence of the magnetostriction on the magnetization. At the same time, when the stress is present, the magnetization is in turn coupled to the behavior of the part of the magnetostriction associated with domain moment rotation.

We have formulated an expression for the magnetostriction and have compared numerical modeling results for magnetostriction hysteresis to experimental results.

Although some features of the magnetostriction in iron and steel still need additional explanation, the main features of the magnetostriction have been accounted for. These include liftoff (failure of the magnetostriction to return to its value in the demagnetized state as the hysteresis loop is cycled) and a magnetostriction increase after flux density B reaches its maximum and starts to decrease. The fact that hysteresis exists in λ versus B is an indication that λ depends on H as well as M . This extra dependence of λ on H is a result of irreversible domain wall motion.

It should be noted that the formulation is a macro-magnetic, multi-domain formulation and yields zero magnetostriction in the demagnetized specimen, unlike the single-domain results for which the magnetostriction is a constant.

ACKNOWLEDGMENTS

The authors are grateful for helpful suggestions made by S. W. Rubin and L. A. Riley. Their assistance in some of the computer calculations is also appreciated.

REFERENCES

- [1] J. P. Joule, "On a new class of magnetic forces," *Ann. Electr. Magn. Chem.*, vol. 8, pp. 219–224, 1842.
- [2] J. C. Maxwell, *Electricity and Magnetism*, London: Oxford, 1873.
- [3] G. Finzi, "On hysteresis in the presence of alternating currents," *Electrician*, vol. 26, pp. 672–673, 1891.
- [4] C. P. Steinmetz, "On the law of hysteresis," *Trans. Am. Inst. Elec. Engrs.*, vol. 9, pp. 3–51, 1892.
- [5] R. M. Bozorth, *Ferromagnetism*, Van Nostrand, pp. 507–514, 1951.
- [6] —, *Ferromagnetism*, Van Nostrand, pp. 655–668, 1951.

- [7] F. C. Trutt, E. A. Erdelyi, and R. E. Hopkins, "Representation of the magnetization characteristic of DC machines for computer use," *IEEE Trans. Power Appl. Sys.*, vol. PAS-87, no. 3, pp. 665-669, Mar. 1968.
- [8] G. F. T. Widger, "Representation of magnetisation curves over extensive range by rational fraction approximation," *Proc. Inst. Electr. Eng.*, vol. 116, no. 1, pp. 156-160, Jan. 1969.
- [9] W. K. MacFayden, R. R. S. Simpson, R. D. Slater, and W. S. Wood, "Representation of magnetisation curves by exponential series," *Proc. IEE*, vol. 120, no. 8, pp. 902-904, Aug. 1973.
- [10] J. R. Brauer, "Simple equations for the magnetization and reluctivity curves of steel," *IEEE Trans. Magn.*, vol. MAG-11, p. 81, Jan. 1975.
- [11] J. Rivas, J. M. Zamorro, E. Martin, and C. Pereira, "Simple approximation for magnetization curves and hysteresis loops," *IEEE Trans. Magn.*, vol. MAG-17, no. 4, pp. 1498-1502, July 1981.
- [12] F. Preisach, "On magnetic lag," *Zeit. fur Physik*, vol. 94, pp. 277-302, 1935.
- [13] R. M. del Vecchio, "An efficient procedure for modeling complex hysteresis processes in ferromagnetic materials," *IEEE Trans. Magn.*, vol. MAG-16, no. 5, pp. 809-811, Sept. 1980.
- [14] M. A. Rahman, M. Poloujadoff, R. D. Jackson, J. Perrard, and S. D. Gowda, "Improved algorithms for digital simulation of hysteresis processes in semi-hard magnetic materials," *IEEE Trans. Magn.*, vol. MAG-17, no. 6, pp. 3253-3255, Nov. 1981.
- [15] T. Doong and I. D. Mayergoyz, "On numerical implementation of hysteresis models," *IEEE Trans. Magn.*, vol. MAG-21, no. 5, pp. 1853-1855, Sept. 1985.
- [16] I. D. Mayergoyz and G. Friedman, "Generalized Preisach model of hysteresis," *IEEE Trans. Magn.*, vol. 24, no. 1, pp. 212-217, Jan. 1988.
- [17] I. D. Mayergoyz, "Dynamic Preisach models of hysteresis," *IEEE Trans. Magn.*, vol. 24, no. 6, pp. 2925-2927, Nov. 1988.
- [18] I. D. Mayergoyz and G. Friedman, "Identification problem for 3-D anisotropic Preisach model of vector hysteresis," *IEEE Trans. Magn.*, vol. 24, no. 6, pp. 2928-2930, Nov. 1988.
- [19] J. B. Restorff, H. T. Savage, A. E. Clark, and M. Wun-Fogle, "Preisach diagrams of hysteresis in terfenol," *J. Appl. Phys.*, vol. 67, no. 9, pp. 5016-5018, May 1, 1990.
- [20] L. Rayleigh, "The behavior of iron and steel under the operation of feeble magnetic forces," *Phil. Mag.*, vol. 23, pp. 225-245, 1867.
- [21] D. C. Jiles and D. L. Atherton, "Ferromagnetic hysteresis," *IEEE Trans. Magn.*, vol. MAG-19, no. 5, pp. 2183-2185, Sept. 1983.
- [22] D. C. Jiles and D. L. Atherton, "Theory of ferromagnetic hysteresis," *J. Appl. Phys.*, vol. 55, no. 6, pp. 2115-2120, Mar. 15, 1984.
- [23] D. C. Jiles and D. L. Atherton, "Theory of the magnetization process in ferromagnets and its application to the magnetomechanical effect," *J. Phys. D*, vol. 17, pp. 1265-1281, 1984.
- [24] D. C. Jiles and D. L. Atherton, "Theory of ferromagnetic hysteresis," *J. Magn. Magn. Mater.*, vol. 61, pp. 48-60, 1986.
- [25] D. C. Jiles, J. B. Thoele, and M. K. Devine, "Numerical determination of hysteresis parameters for the modeling of magnetic properties using the theory of ferromagnetic hysteresis," *IEEE Trans. Magn.*, vol. 28, no. 1, pp. 27-35, Jan. 1992.
- [26] M. J. Sablik, H. Kwun, G. L. Burkhardt, and D. C. Jiles, "Model for the effect of tensile and compressive stress on ferromagnetic hysteresis," *J. Appl. Phys.*, vol. 61, no. 8, pp. 3799-3801, 1987.
- [27] M. J. Sablik, G. L. Burkhardt, H. Kwun, and D. C. Jiles, "A model for the effect of stress on the low-frequency harmonic content of the magnetic induction in ferromagnetic materials," *J. Appl. Phys.*, vol. 63, no. 8, pp. 3930-3932, 1988.
- [28] M. J. Sablik and D. C. Jiles, "A model for magnetostriction hysteresis," *J. Appl. Phys.*, vol. 64, no. 10, pp. 5402-5404, Nov. 15, 1988.
- [29] M. J. Sablik, W. L. Rollwitz, and D. C. Jiles, "A model for magabsorption as an NDE tool for stress measurement," *Proc. 17th Symposium on NDE*, San Antonio, TX, Apr. 17-20, 1989, p. 212-223. (NTIAC, Southwest Research Institute, San Antonio, TX, 1989).
- [30] M. J. Sablik, "Modeling stress dependence of magnetic properties for NDE of steels," *Nondestructive Testing and Eval.*, vol. 5, pp. 49-65, 1989.
- [31] M. J. Sablik, D. C. Jiles, and L. Barghout, "First principles approach to magnetostrictive hysteresis," *J. Appl. Phys.*, vol. 67, no. 9, p. 5019, May 1, 1990 (abstract only).
- [32] M. J. Sablik and H. Kwun, "Hysteretic model for Barkhausen noise and the magnetically induced velocity change of ultrasonic waves in ferromagnets under stress," *J. Appl. Phys.*, vol. 69, no. 8, pp. 5791-5793, Apr. 15, 1991.
- [33] M. J. Sablik and S. W. Rubin, "Relationship of magnetostrictive hysteresis to the ΔE effect," *J. Magn. Magn. Mater.*, vol. 104-107, pp. 392-394, 1992.
- [34] P. Garikepati, T. T. Chang, and D. C. Jiles, "Theory of ferromagnetic hysteresis: evaluation of stress from hysteresis curves," *IEEE Trans. Magn.*, vol. 24, no. 6, pp. 2922-2924, Nov. 1988.
- [35] R. M. Bozorth, loc. cit., pp. 538-546.
- [36] B. D. Cullity, *Introduction to Magnetic Materials*, Reading, Massachusetts: Addison-Wesley, p. 283, 1972.
- [37] D. C. Jiles, *Introduction to Magnetism and Magnetic Materials*, pp. 130-134, Chapman and Hall, 1991.
- [38] D. C. Jiles and S. Hariharan, "Interpretation of the magnetization mechanism in terfenol-D using Barkhausen pulse-height analysis and irreversible magnetostriction," *J. Appl. Phys.*, vol. 67, no. 9, pp. 5013-5015, May 1, 1990.
- [39] R. M. Spano, K. B. Hathaway, and H. T. Savage, "Magnetostriction and magnetic anisotropy of field-annealed Metglas 2605 alloys via dc M-H Loop measurement under stress," *J. Appl. Phys.*, vol. 53, no. 3, pp. 2667-2669, Mar. 1982.
- [40] S. Chikazumi and S. H. Charap, *Physics of Magnetism*, Malabar, Florida: Krieger, p. 163, 1984.
- [41] —, *Physics of Magnetism*, Malabar, Florida: Krieger, pp. 170-173, 1984.
- [42] A. Bienkowski and J. Kulikowski, "The dependence of Villari effect in ferrites on their magnetocrystalline properties and magnetostriction," *J. Magn. Magn. Mater.*, vol. 26, pp. 292-294, 1982.
- [43] D. L. Atherton, T. S. Rao, V. De Sa, and M. Schönbachler, "Thermodynamic correlation tests between magnetostrictive and magnetomechanical effects in 2% Mn pipeline steel," *IEEE Trans. Magn.*, vol. 24, pp. 2177-2180, Sept. 1980.
- [44] B. D. Cullity, loc. cit., p. 277.
- [45] E. Villari, "Change of magnetization by tension and by electric current," *Ann. Phys. Chem.*, vol. 126, p. 87, 1865.
- [46] J. A. Ewing, *Magnetic Induction in Iron and Other Metals*, New York: Van Nostrand, pp. 198-200, 1892.
- [47] C. S. Schneider, P. Y. Cannell, and K. T. Watts, "Magnetoelasticity for large stresses," *IEEE Trans. Magnetics*, Vol. 28, p. 2626, 1992.

Martin J. Sablik (M-'80) received the Ph.D. in physics from Fordham University, Bronx, NY in 1972, after completing the M.S. in physics with the University of Kentucky, Lexington, KY (1965) and the B.A. in physics with Cornell University, Ithaca, NY, (1960).

He taught physics at Fairleigh Dickinson University from 1967-1980 and achieved the rank of Associate Professor. Since 1980, he has been doing applied physics research at Southwest Research Institute, San Antonio, TX, where his present rank is Staff Scientist. He has authored or co-authored approximately 100 scientific papers and technical presentations, and has a patent and several patent applications.

Dr. Sablik is a member of the American Physical Society, the American Society for Nondestructive Testing, the American Geophysical Union, and the American Association of Physics Teachers.

David C. Jiles (M'83-SM'89) received the Ph.D. degree in applied physics from the University of Hull, Hull, England, in 1979, and studied at Victoria University, New Zealand, and Queen's University, Canada.

He joined the Ames Laboratory, Iowa State University, in 1984 and the Center for NDE in 1986. He is currently a Senior Physicist with Iowa State University Institute for Physical Research and Technology and Professor of Materials Science and Engineering and Professor of Electrical Engineering. He is the author of over 150 technical papers and presentations, and the author of the book, *Introduction of Magnetism and Magnetic Materials* (1990).

Dr. Jiles is a Fellow of the Institute of Physics and a member of the American Physical Society, the American Society for Materials, the Metallurgical Society, and the American Society for Nondestructive Testing. He is a registered professional engineer and a registered Chartered Engineer, serves as a consultant for several companies both in North America and Europe, and was awarded a higher doctorate in physics in 1990 by the University of Birmingham for his work on the magnetic and electronic properties of metals.